

ARTICLE

Open Access

Loss-induced nonreciprocity

Xinyao Huang¹, Cuicui Lu^{2,3}, Chao Liang¹, Honggeng Tao¹ and Yong-Chun Liu^{1,4}

Abstract

Nonreciprocity is important in both optical information processing and topological photonics studies. Conventional principles for realizing nonreciprocity rely on magnetic fields, spatiotemporal modulation, or nonlinearity. Here we propose a generic principle for generating nonreciprocity by taking advantage of energy loss, which is usually regarded as harmful. The loss in a resonance mode induces a phase lag, which is independent of the energy transmission direction. When multichannel lossy resonance modes are combined, the resulting interference gives rise to nonreciprocity, with different coupling strengths for the forward and backward directions, and unidirectional energy transmission. This study opens a new avenue for the design of nonreciprocal devices without stringent requirements.

Introduction

Optical nonreciprocity, which prohibits a light field from returning along its original path after passing through an optical system in one direction, implying the breaking of the Lorentz reciprocity theorem, is crucially important for both fundamental studies and applied sciences^{1–3}. For example, nonreciprocal devices, such as optical isolators¹, optical circulators⁴, and directional amplifiers⁵, play important roles in optical communication and optical information processing. Moreover, the topological properties exhibited by nonreciprocal devices make them promising platforms for studying topological photonics^{6,7} and chiral quantum optics⁸. To date, a number of approaches have been suggested for generating nonreciprocity, including the use of parity-time (PT)-symmetric nonlinear cavities^{9,10}, spinning resonators^{11,12}, optomechanical interactions^{13–20}, cavity magnonic interactions²¹, effective gauge fields^{22,23}, and the thermal motion of hot atoms^{24,25}. Despite these achievements, the basic principles for realizing optical nonreciprocity remain limited as a result of the time-reversal symmetry

and linear nature of Maxwell's equations. The existing approaches can be grouped into three categories with the following requirements^{1–3}: (i) magnetic-field-induced breaking of time-reversal symmetry^{26–29}, (ii) spatiotemporal modulation of system permittivity^{30–36}, and (iii) nonlinearity^{37,38}. However, these principles either encounter difficulties in integration³⁹, require stringent experimental conditions⁴⁰, or have limited performance³⁸. Therefore, it is crucial to break the Lorentz reciprocity theorem by going beyond these approaches.

Here we devise a new principle for realizing optical nonreciprocity by making use of loss. Although it is obvious that loss breaks time-reversal symmetry, it is generally believed that loss cannot lead to optical nonreciprocity as a result of restricted time-reversal symmetry^{2,3}, in which the field amplitudes are reduced while the field ratios are conserved. However, we show that loss under multiple channels with interference gives rise to optical nonreciprocity. The basic principle is that the phase lag induced by loss, which is independent of the energy propagation direction, results in different interference outcomes for the forward and backward directions. In our scheme, neither a magnetic field, the spatiotemporal modulation of permittivity nor nonlinearity is required. On the contrary, the resource we take advantage of is simply energy loss, which is regarded as harmful and undesirable in most studies. This is also different from PT-symmetric schemes in which the

Correspondence: Yong-Chun Liu (ycliu@tsinghua.edu.cn)

¹State Key Laboratory of Low-Dimensional Quantum Physics, Department of Physics, Tsinghua University, Beijing 100084, China

²Key Laboratory of Advanced Optoelectronic Quantum Architecture and Measurements of Ministry of Education, Beijing Key Laboratory of Nanophotonics and Ultrafine Optoelectronic Systems, School of Physics, Beijing Institute of Technology, Beijing 100081, China

Full list of author information is available at the end of the article

© The Author(s) 2021



Open Access This article is licensed under a Creative Commons Attribution 4.0 International License, which permits use, sharing, adaptation, distribution and reproduction in any medium or format, as long as you give appropriate credit to the original author(s) and the source, provide a link to the Creative Commons license, and indicate if changes were made. The images or other third party material in this article are included in the article's Creative Commons license, unless indicated otherwise in a credit line to the material. If material is not included in the article's Creative Commons license and your intended use is not permitted by statutory regulation or exceeds the permitted use, you will need to obtain permission directly from the copyright holder. To view a copy of this license, visit <http://creativecommons.org/licenses/by/4.0/>.

nonreciprocity originates from nonlinear gain with saturation. Our scheme is universal for a variety of physical systems, such as optical cavities and waveguides. This study paves the way for the observation of nonreciprocity and corresponding device design in lossy systems without stringent conditions, and provides opportunities for studying chiral and topological properties in systems with lossy coupling.

Results

As illustrated in Fig. 1a, we consider a generic system in which an array of main resonance modes a_m ($m = 1, 2, \dots, M$) are linked by a series of connecting modes $c_m^{(n)}$ ($n = 1, 2, \dots, N$) with decay rates $\kappa_m^{(n)}$. This model can be implemented in a variety of systems, such as optical cavities⁴¹, superconducting circuits⁴², mechanical resonators⁴³, and atomic ensembles⁴⁴. In the frame rotating at the input laser frequency ω_1 , the system Hamiltonian is given by ($\hbar = 1$)

$$H = - \sum_{m=1}^M \Delta_m a_m^\dagger a_m - \sum_{m=1}^{M-1} \sum_{n=1}^N \Delta_m^{(n)} c_m^{(n)\dagger} c_m^{(n)} + \sum_{m=1}^{M-1} \sum_{n=1}^N (g_{L,m}^{(n)} a_m^\dagger + g_{R,m}^{(n)} a_{m+1}^\dagger) c_m^{(n)} + H.c. \quad (1)$$

where $\Delta_m \equiv \omega_1 - \omega_m$ and $\Delta_m^{(n)} \equiv \omega_1 - \omega_m^{(n)}$ represent the detunings, with ω_m ($\omega_m^{(n)}$) being the resonance frequency of mode a_m ($c_m^{(n)}$) and $g_{L,m}^{(n)}$ ($g_{R,m}^{(n)}$) being the coupling coefficient between a_m (a_{m+1}) and $c_m^{(n)}$. Here, the indices of the main (connecting) modes are denoted by subscripts (superscripts in parentheses) to avoid confusion.

In the above model, N connecting modes are required to realize N -channel coupling between a_m and a_{m+1} . As sketched in Fig. 1b, this multichannel coupling can also be realized by using only one connecting mode c_m with synthetic frequency dimensions, where N pairs of coupling detunings $\delta_{L/R,m}^{(n)}$ play the role of N coupling channels. In this case, the system Hamiltonian is expressed as

$$H = - \sum_{m=1}^M \Delta_m a_m^\dagger a_m - \sum_{m=1}^{M-1} \Delta_m c_m^\dagger c_m + \sum_{m=1}^{M-1} \sum_{n=1}^N [(g_{L,m}^{(n)} e^{i\delta_{L,m}^{(n)} t} a_m^\dagger + g_{R,m}^{(n)} e^{i\delta_{R,m}^{(n)} t} a_{m+1}^\dagger) c_m + H.c.]$$

where $\Delta_m^c \equiv \omega_1 - \omega_m^c$ is the detuning of the connecting mode c_m . By expressing the connecting mode as $c_m = \sum_{n=1}^N (c_{L,m}^{(n)} e^{-i\delta_{L,m}^{(n)} t} + c_{R,m}^{(n)} e^{-i\delta_{R,m}^{(n)} t})$, where the $c_{L/R,m}^{(n)}$ are the components corresponding to the coupling detunings $\delta_{L/R,m}^{(n)}$, this Hamiltonian can ultimately be reduced to Eq. (1) under the rotating-wave approximation (see the Supplementary Information for details).

When the detunings $\Delta_m^{(n)}$ or decay rates $\kappa_m^{(n)}$ of the connecting modes are much larger than the coupling rates ($|\Delta_m^{(n)} + i\kappa_m^{(n)}/2| \gg |g_{L/R,m}^{(n)}|$), the connecting modes $c_m^{(n)}$ can be adiabatically eliminated^{45,46}, leading to an effective non-Hermitian Hamiltonian $H_{\text{eff}} = H_{\text{eff}}^0 + H_{\text{eff}}^{\text{int}}$ (see the Supplementary Information for details). Here, $H_{\text{eff}}^0 = - \sum_{m=1}^M (\Delta_m + i\gamma_m/2 + \Omega_m) a_m^\dagger a_m$ is the free-energy term, with γ_m being the intrinsic linewidth of mode a_m and $\Omega_m = - \sum_{n=1}^N \left[|g_{L,m}^{(n)}|^2 / (\Delta_m^{(n)} + i\kappa_m^{(n)}/2) + |g_{R,m-1}^{(n)}|^2 / (\Delta_{m-1}^{(n)} + i\kappa_{m-1}^{(n)}/2) \right]$ being the resonance shift and broadening; $H_{\text{eff}}^{\text{int}}$ is the interaction term, given by

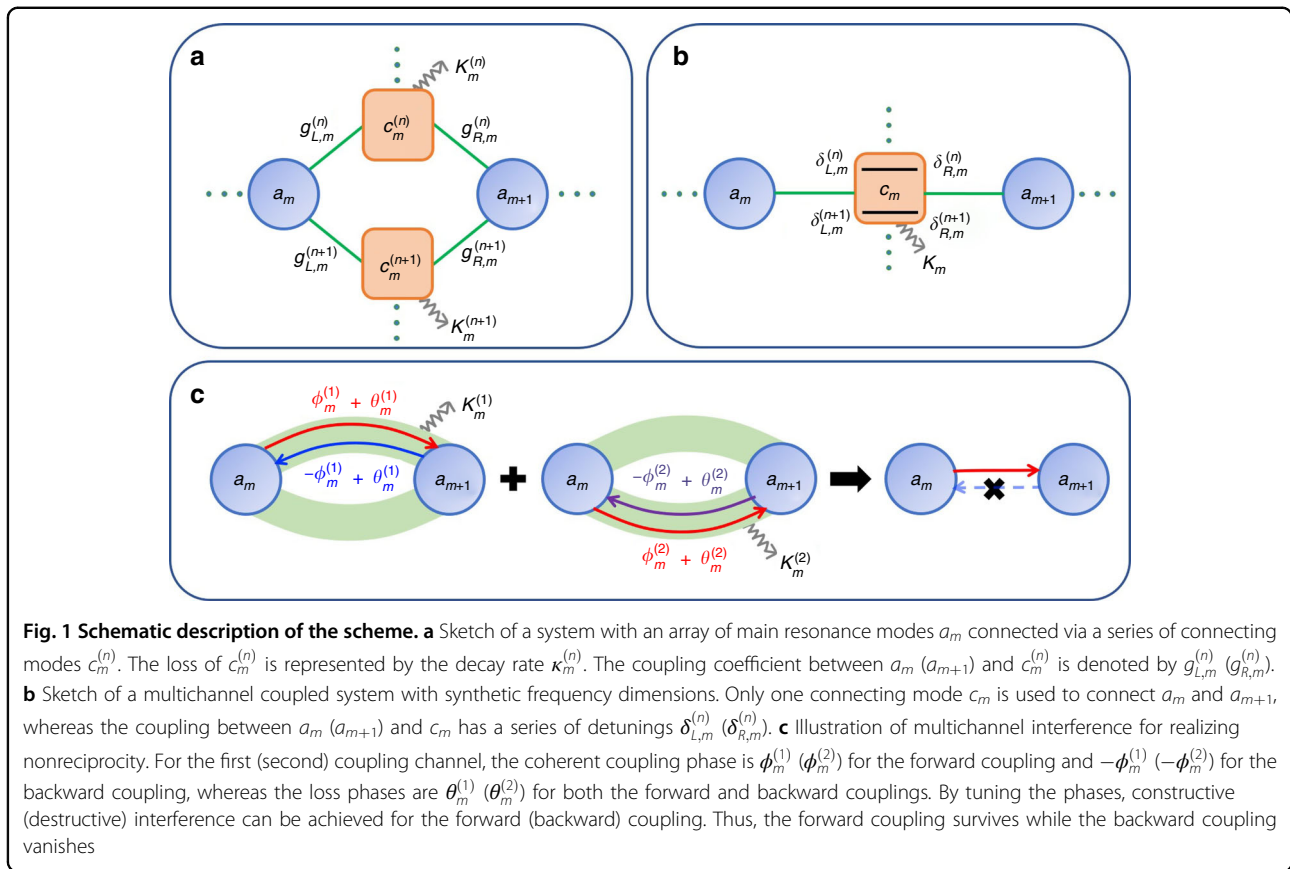
$$H_{\text{eff}}^{\text{int}} = \sum_{m=1}^{M-1} (h_{m+1,m} a_{m+1}^\dagger a_m + h_{m,m+1} a_m^\dagger a_{m+1}) \quad (2)$$

$$h_{m+1,m} = \sum_{n=1}^N G_m^{(n)} e^{-i\phi_m^{(n)} - i\theta_m^{(n)}} \quad (2)$$

$$h_{m,m+1} = \sum_{n=1}^N G_m^{(n)} e^{i\phi_m^{(n)} - i\theta_m^{(n)}}$$

where $h_{m+1,m}$ ($h_{m,m+1}$) is the effective coupling coefficient for the forward (backward) direction between a_m and a_{m+1} . It is seen that the total effective coupling coefficient is a sum of the effective coupling coefficients for each coupling channel. For the n -th channel, the amplitude of the effective coupling coefficient is $G_m^{(n)} \equiv |g_{L,m}^{(n)} g_{R,m}^{(n)}| / \sqrt{\Delta_m^{(n)2} + \kappa_m^{(n)2}/4}$, whereas the phase factors include two components: $\phi_m^{(n)}$ and $\theta_m^{(n)}$. The first component, $\phi_m^{(n)} \equiv \arg(g_{L,m}^{(n)} g_{R,m}^{(n)*})$, refers to the coherent coupling phase, which changes its sign when the coupling direction is reversed as a result of energy conservation. The second component, $\theta_m^{(n)} \equiv \arg(\Delta_m^{(n)} + i\kappa_m^{(n)}/2)$, represents the phase lag induced by loss (the loss phase). It is noteworthy that this loss phase is determined only by the loss-detuning ratio, not by the coupling direction, as the losses play the same role for both the forward and backward couplings.

In the absence of losses, i.e., when $\kappa_m^{(n)} = 0$ and thus $\theta_m^{(n)} = 0$, $h_{m,m+1}$ and $h_{m+1,m}$ are complex conjugates, and $H_{\text{eff}}^{\text{int}}$ is Hermitian. In the presence of losses, the phase lag $\theta_m^{(n)}$ yields a non-Hermitian $H_{\text{eff}}^{\text{int}}$ with $h_{m,m+1} \neq h_{m+1,m}^*$. When only one loss channel exists ($N = 1$), the effective coupling amplitudes for the forward and backward couplings are still the same, i.e., $|h_{m,m+1}| = |h_{m+1,m}|$, meaning that a nonreciprocal energy flow does not exist. This is consistent with the conclusion in the previous literature^{2,3}, in which lossy systems are regarded as reciprocal in terms of restricted time-reversal symmetry. However,



when more than one channel exists, the interference between different channels ultimately leads to unequal effective coupling amplitudes for the forward and backward couplings, i.e., $|h_{m,m+1}| \neq |h_{m+1,m}|$ for $N \geq 2$. As depicted in Fig. 1c, the existence of the loss phase ensures that the interference properties are different for the forward and backward couplings. By tuning the phases, the forward coupling can be made to experience constructive interference, whereas the backward coupling will undergo destructive interference, leading to a nonzero forward coupling strength but a backward coupling strength of zero. This asymmetric coupling leads to an asymmetric scattering matrix (see the Supplementary Information for details), which indicates that the Lorentz reciprocity is broken¹. Thus, nonreciprocity can be realized in a lossy system with multichannel interference. It is noteworthy that neither a magnetic field, the spatiotemporal modulation of permittivity, nor nonlinearity is required, and the nonreciprocity originates purely from the losses, which break the time-reversal symmetry.

Without loss of generality, in the following, we consider a two-channel situation ($N = 2$). To realize complete nonreciprocity, the amplitudes of the coupling coefficients for the two channels should be the same,

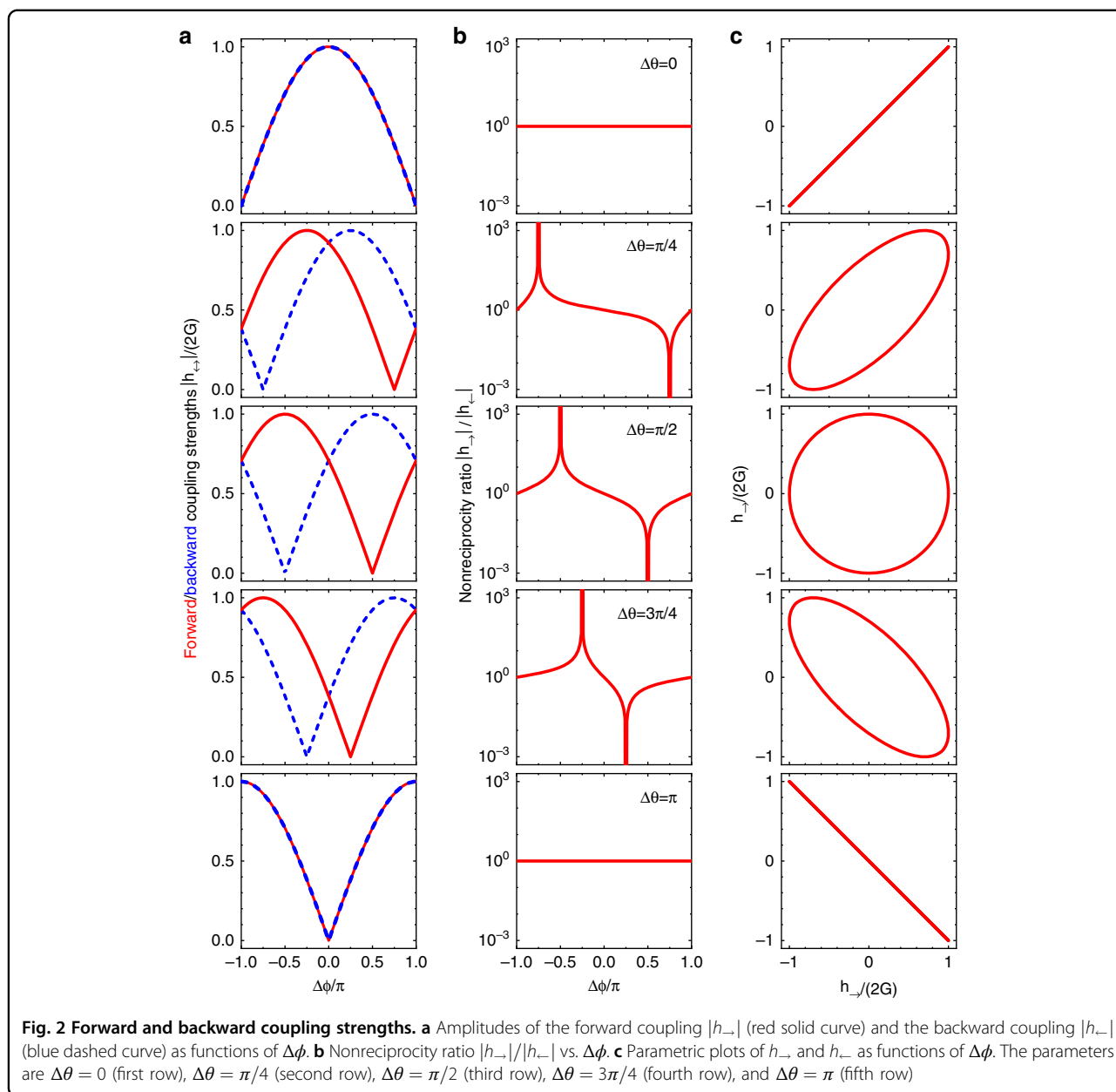
i.e., $G_m^{(1)} = G_m^{(2)}$ (denoted by G in the following), so that complete destructive interference can be achieved. In this case, the forward and backward coupling coefficients are given by

$$h_{\pm} = 2Ge^{\mp i\bar{\phi} - i\bar{\theta}} \cos \frac{\Delta\phi \pm \Delta\theta}{2} \tag{3}$$

where h_{\pm} (h_{\pm}) is short for $h_{m+1,m}$ ($h_{m,m+1}$), $\Delta\phi = \phi_m^{(2)} - \phi_m^{(1)}$ is the difference between the coherent coupling phases for the two channels, $\Delta\theta = \theta_m^{(2)} - \theta_m^{(1)}$ is the loss phase difference, and $\bar{\phi} = (\phi_m^{(1)} + \phi_m^{(2)})/2$ and $\bar{\theta} = (\theta_m^{(1)} + \theta_m^{(2)})/2$ are the corresponding average phases. Here, the subscripts “ m ” for the m -th main mode are omitted for convenience, as we mainly focus on the $M = 2$ case. It is clearly revealed that the phase difference leads to distinct interference patterns for the forward and backward couplings. The conditions for unidirectional nonreciprocal coupling are given by

$$\begin{aligned} \Delta\phi \mp \Delta\theta &= \pi + 2k\pi \\ \Delta\phi \neq p\pi, \Delta\theta &\neq q\pi \end{aligned} \tag{4}$$

where k , p , and q are integers. Here, “ $-$ ” corresponds to unidirectional forward coupling with $|h_{\pm}| \neq 0$ and

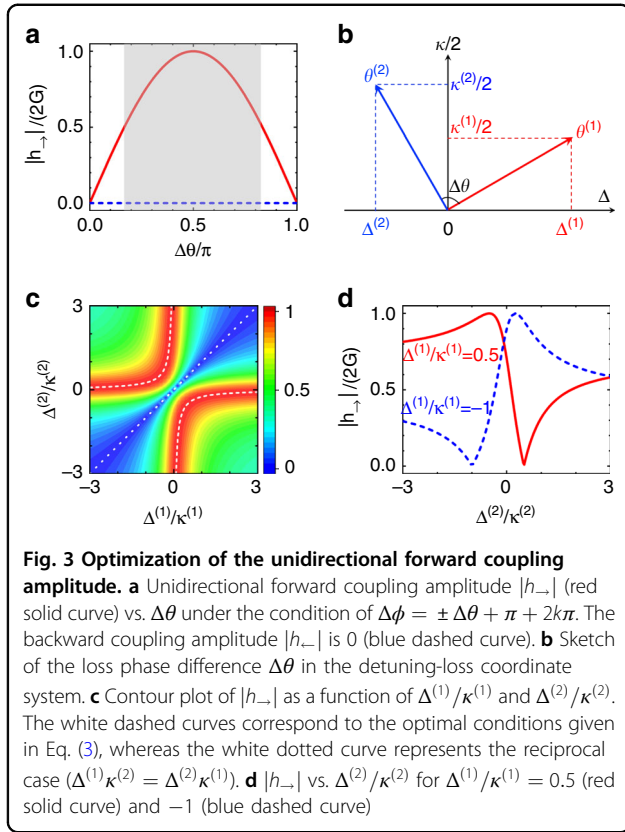


$|h_{\leftarrow}| = 0$, whereas “+” corresponds to unidirectional backward coupling with $|h_{\rightarrow}| = 0$ and $|h_{\leftarrow}| \neq 0$.

In Fig. 2a, we plot the amplitudes of the forward and backward couplings $|h_{\pm}|$ as functions of $\Delta\phi$ for various loss phase differences $\Delta\theta$. When $\Delta\theta = 0$ or π , the curves of $|h_{\pm}|$ coincide and thus, nonreciprocity is not achievable. However, for other values of $\Delta\theta$, the difference between $|h_{\rightarrow}|$ and $|h_{\leftarrow}|$ becomes significant. The curves of $|h_{\pm}|$ have the same lineshape, but the positions are shifted to the left (right) by $\Delta\theta$, showing that nonreciprocity can be realized. As depicted in Fig. 2b, the nonreciprocity ratio $|h_{\rightarrow}|/|h_{\leftarrow}|$ reaches a maximum/minimum when $\Delta\phi = \pm(\Delta\theta - \pi)$, in agreement with Eq. (4). For example,

$\Delta\theta = \pi/2$ and $\Delta\phi = -\pi/2$ ($\pi/2$) lead to unidirectional forward (backward) coupling (third row of Fig. 2). The nonreciprocal properties can also be illustrated by the trajectories in the parameter space expanded by h_{\rightarrow} and h_{\leftarrow} , as shown in Fig. 2c. The loss phase difference $\Delta\theta$ exactly matches the relative phase lag between h_{\rightarrow} and h_{\leftarrow} , where $\Delta\theta = 0$ and π correspond to linear trajectories without nonreciprocity and $\Delta\theta = \pi/2$ corresponds to a circular trajectory with the most prominent nonreciprocity, whereas for other values, the trajectories are ellipses with modest nonreciprocity.

Under the unidirectional forward coupling condition with $\Delta\phi = \Delta\theta + \pi + 2k\pi$, the amplitude of the forward



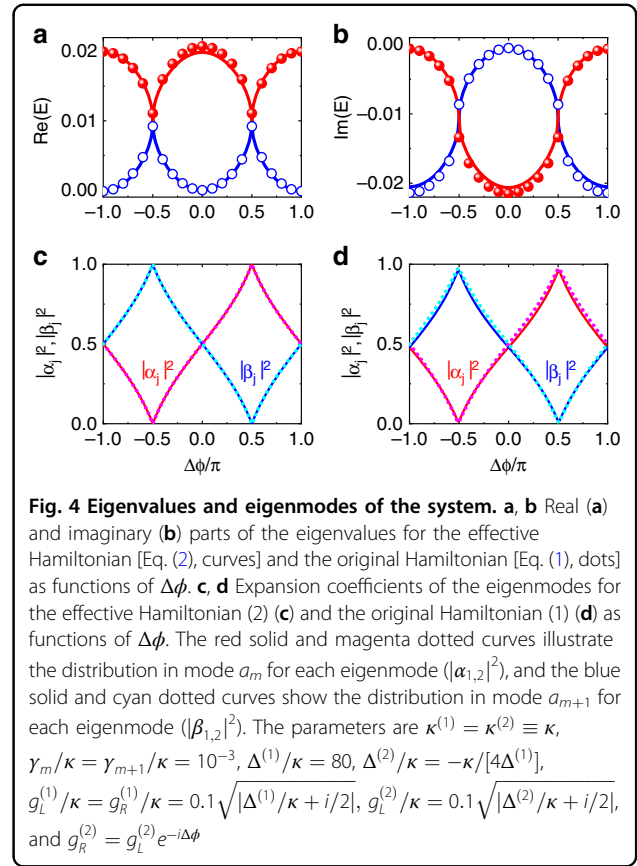
coupling coefficient is given by

$$|h_{-}| = 2G|\sin\Delta\theta| \tag{5}$$

As illustrated in Fig. 3a, the loss phase difference $\Delta\theta$ strongly determines the unidirectional coupling strength. The best performance is achievable for $\Delta\theta = \pi/2$, with the corresponding maximum being $|h_{-}|_{\max} = 2G$. It is noteworthy that the unidirectional coupling strength can remain large over a broad range of $\Delta\theta$, with the full width at half maximum being $2\pi/3$ (shaded region). By expressing $\Delta\theta$ in terms of the detunings and losses for the two coupling channels (Fig. 3b), we obtain $\tan\Delta\theta = 2[\Delta^{(1)}/\kappa^{(2)} - \Delta^{(2)}/\kappa^{(1)}]/[4\Delta^{(1)}/\kappa^{(2)} + \kappa^{(1)}/\kappa^{(2)}]$. Thus, the optimal condition can be re-expressed as

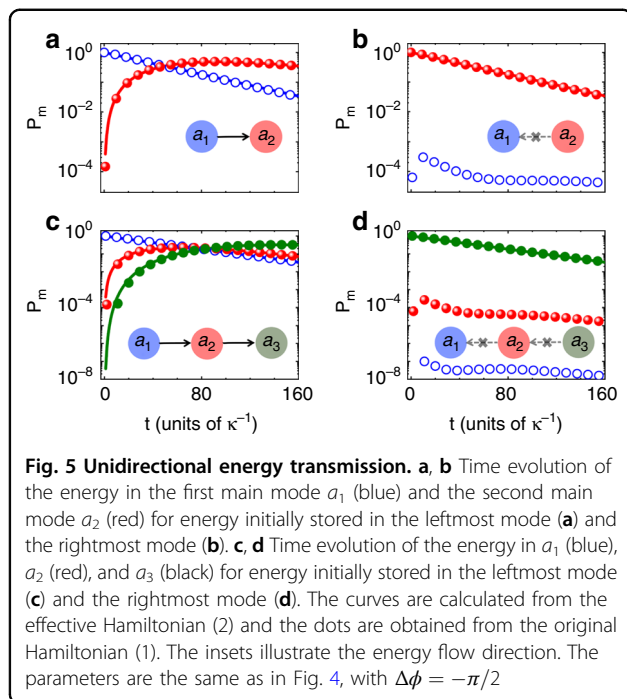
$$\frac{\Delta^{(1)}/\kappa^{(2)}}{\kappa^{(1)}/\kappa^{(2)}} = -\frac{1}{4} \tag{6}$$

whereas the condition for vanishing nonreciprocity is $\Delta^{(1)}/\kappa^{(2)} = \Delta^{(2)}/\kappa^{(1)}$. The contour map of $|h_{-}|$ as a function of $\Delta^{(1)}/\kappa^{(1)}$ and $\Delta^{(2)}/\kappa^{(2)}$ is plotted in Fig. 3c, and typical curves for $|h_{-}|$ as a function of $\Delta^{(2)}/\kappa^{(2)}$ with a fixed $\Delta^{(1)}/\kappa^{(1)}$ are plotted in Fig. 3d. These figures show that the parameter ranges for achieving a large $|h_{-}|$ are very broad. For a pure lossy system, two detunings with



opposite signs are preferred, i.e., in one channel, the connecting mode is red detuned, whereas in the other channel the connecting mode should be blue detuned.

The nonreciprocity can also be reflected in the eigenvalues and eigenmodes of the system. In Fig. 4, we plot the real and imaginary parts of the energy eigenvalues and the expansion coefficients of the eigenmodes (defined as $e_j = \alpha_j a_m + \beta_j a_{m+1}$, $j = 1, 2$) as functions of $\Delta\phi$ for $\Delta\theta = \pi/2$ (corresponding to the third row in Fig. 2). For the reciprocal cases ($\Delta\phi = 0, \pm\pi$), the eigenvalues are split to the maximum extent, whereas the eigenmodes are equally weighted superpositions of a_m and a_{m+1} . As the nonreciprocity ratio increases, for instance, $\Delta\phi$ varies from 0 to $\pm\pi/2$, the eigenvalue splitting becomes smaller, and the eigenmodes tend to be more localized in one of the main modes. For the completely nonreciprocal points, $\Delta\phi = \pm\pi/2$, the eigenvalues become degenerate, accompanied by the coalescence of the eigenmodes, which are the features of exceptional points⁴⁷. This is because the unidirectional nonreciprocal coupling causes one of the modes to be unstable and only one mode survives. For instance, $\Delta\phi = -\pi/2$ corresponds to a unidirectional forward coupling, meaning that the energy irreversibly flows from a_m to a_{m+1} and, thus, only a_{m+1} survives as the eigenmode ($|\beta_j| = 1$). It is worth noting that the results



obtained by diagonalizing the effective Hamiltonian (2) with adiabatic elimination are consistent with those obtained from the original Hamiltonian (1), as shown in Fig. 4.

A unidirectional nonreciprocal coupling directly gives rise to unidirectional energy transmission between the main resonance modes. In Fig. 5, we plot the typical results of unidirectional energy transmission for two ($M = 2$) and three ($M = 3$) main modes in the case of a forward unidirectional coupling ($|h_{\rightarrow}| \neq 0$ and $|h_{\leftarrow}| = 0$). It is revealed that forward transmission is allowed (Fig. 5a, c), whereas backward transmission is forbidden. The residual backward transmission, which originates from the imperfect adiabatic elimination of the connecting modes, is only 10^{-4} for $M = 2$ and 10^{-8} for $M = 3$ (Fig. 5b, d). The results calculated from the effective Hamiltonian (2) with adiabatic elimination (curves) agree well with those obtained from the original Hamiltonian (1) (dots).

Discussion

Breaking Lorentz reciprocity is a very challenging task due to the time-reversal symmetry and linear nature of Maxwell's equations, and at present, only three routes towards realizing nonreciprocity have been discovered, using a magnetic field, spatiotemporal modulation, or nonlinearity. Although loss breaks the time-reversal symmetry according to the traditional definition of time reversal, it is commonly believed that in classical electrodynamics, only restricted time reversal is valid. In this framework, lossy materials remain lossy under time-reversal transformation and restricted time-reversal symmetry still holds, which implies reciprocity^{2,3}. Here

we demonstrate that nonreciprocity can be achieved by making use of loss combined with multichannel interference. Due to the interference with different loss angles, the field ratios do not remain conserved under time-reversal transformation.

Although PT-symmetric systems also make use of losses^{9,10,48}, it is clear that the nonreciprocity reported in previous PT-symmetric cavity schemes originates from the nonlinear gain saturation effect, i.e., the basic principle used to generate nonreciprocity is nonlinearity^{9,10}. In our scheme, we focus on a pure lossy and linear system, in which neither gain nor nonlinearity is required and the fundamental aspect giving rise to nonlinearity is loss. It is noteworthy that loss is ubiquitous, whereas gain and nonlinearity are not common in optical systems. In addition, we clarify that the above results represent nonreciprocity but not simply asymmetrical power transmission, as the input and output channels both contain a single mode and the scattering matrix is asymmetric (see the Supplementary Information for details), indicating the breaking of Lorentz reciprocity. This can also be verified when we consider the implementation of our scheme by means of an experimentally feasible setup in which single-mode standing-wave photonic crystal cavities are connected by waveguides^{49,50} (see also the Supplementary Information for more details). The forward (backward) energy transmission coefficient can be defined as $T_{\rightarrow} \equiv |\langle a_{m+1}^{\text{out}}/a_m^{\text{in}} \rangle|^2$ ($T_{\leftarrow} \equiv |\langle a_m^{\text{out}}/a_{m+1}^{\text{in}} \rangle|^2$), which is equal to the modular square of the off-diagonal element $S_{m+1,m}$ ($S_{m,m+1}$) of the scattering matrix and proportional to the modular square of the forward (backward) coupling coefficient h_{\rightarrow} (h_{\leftarrow}). Once the forward and backward coupling strengths are tuned to be unequal, the asymmetric scattering matrix leads to asymmetric forward and backward transmission coefficients, yielding nonreciprocity. Moreover, the unidirectional forward (backward) energy transmission coefficient can be maximized to 68.6% by optimizing the system parameters (the detailed derivations can be found in the Supplementary Information), corresponding to a 1.6 dB insertion loss.

In summary, we present the principle of loss-induced nonreciprocity, which is completely different from the existing principles relying on a magnetic field, spatiotemporal modulation, or nonlinearity. We design a coupled-mode model with a series of resonance modes interacting with each other via lossy connecting modes. A lossy mode possesses a phase lag induced by energy loss, which does not depend on the energy transmission direction. The interference between different coupling channels with different loss phases results in different coupling strengths for the forward and backward directions, yielding nonreciprocity. This property can be exactly tuned by matching the coherent coupling phases and loss phases,

which depend on the ratio between the detuning and energy decay rate of the resonance modes. Our model is universal and can be applied to a variety of systems that can be described by resonance modes, such as optical cavities and waveguides, mechanical resonators, and superconducting circuits. Our work provides new opportunities for designing nonreciprocal optical devices and exploring topological properties such as the non-Hermitian skin effect⁵¹ without requiring a magnetic field, spatiotemporal modulation, nonlinearity, or other stringent conditions, and it may also inspire the further exploration of methods of turning harmful effects into resources.

Acknowledgements

This work was supported by the Key-Area Research and Development Program of Guangdong Province (Grant number 2019B030330001) and the National Natural Science Foundation of China (NSFC) (Grant numbers 92050110, 91736106, 11674390, 91836302, 91850117, and 11654003). X.H. is partly supported by the China Postdoctoral Science Foundation (BX20190179 and 2020M670277).

Author details

¹State Key Laboratory of Low-Dimensional Quantum Physics, Department of Physics, Tsinghua University, Beijing 100084, China. ²Key Laboratory of Advanced Optoelectronic Quantum Architecture and Measurements of Ministry of Education, Beijing Key Laboratory of Nanophotonics and Ultrafine Optoelectronic Systems, School of Physics, Beijing Institute of Technology, Beijing 100081, China. ³Collaborative Innovation Center of Light Manipulations and Applications, Shandong Normal University, Jinan 250358, China. ⁴Frontier Science Center for Quantum Information, Beijing 100084, China

Author contributions

Y.L. conceived the idea. Y.L. and X.H. carried out the calculations and wrote the paper. C.L. provided advice and helpful discussions. All authors contributed to the discussion of the results. Y.L. supervised the project.

Conflict of interest

The authors declare that they have no conflict of interest.

The online version contains Supplementary Materials available at <https://doi.org/10.1038/s41377-021-00464-2>.

Received: 21 July 2020 Revised: 8 December 2020 Accepted: 5 January 2021

Published online: 04 February 2021

References

- Jalas, D. et al. What is – and what is not – an optical isolator. *Nat. Photonics* **7**, 579–582 (2013).
- Caloz, C. et al. Electromagnetic nonreciprocity. *Phys. Rev. Appl.* **10**, 047001 (2018).
- Asadchy, V. S. et al. Tutorial on electromagnetic nonreciprocity and its origins. *Proc. IEEE* **108**, 1684–1727 (2020).
- Kamal, A., Clarke, J. & Devoret, M. H. Noiseless non-reciprocity in a parametric active device. *Nat. Phys.* **7**, 311–315 (2011).
- Malz, D. et al. Quantum-limited directional amplifiers with optomechanics. *Phys. Rev. Lett.* **120**, 023601 (2018).
- Wang, Z. et al. Observation of unidirectional backscattering-immune topological electromagnetic states. *Nature* **461**, 772–775 (2009).
- Bliokh, K. Y., Smirnova, D. & Nori, F. Quantum spin Hall effect of light. *Science* **348**, 1448–1451 (2015).
- Lodahl, P. et al. Chiral quantum optics. *Nature* **541**, 473–480 (2017).
- Peng, B. et al. Parity-time-symmetric whispering-gallery microcavities. *Nat. Phys.* **10**, 394–398 (2014).
- Chang, L. et al. Parity-time symmetry and variable optical isolation in active-passive-coupled microresonators. *Nat. Photonics* **8**, 524–529 (2014).
- Maayani, S. et al. Flying couplers above spinning resonators generate irreversible refraction. *Nature* **558**, 569–572 (2018).
- Huang, R. et al. Nonreciprocal photon blockade. *Phys. Rev. Lett.* **121**, 153601 (2018).
- Barzanjeh, S. et al. Mechanical on-chip microwave circulator. *Nat. Commun.* **8**, 953 (2017).
- Kim, J. et al. Non-reciprocal Brillouin scattering induced transparency. *Nat. Phys.* **11**, 275–280 (2015).
- Shen, Z. et al. Experimental realization of optomechanically induced non-reciprocity. *Nat. Photonics* **10**, 657–661 (2016).
- Ruesink, F. et al. Nonreciprocity and magnetic-free isolation based on optomechanical interactions. *Nat. Commun.* **7**, 13662 (2016).
- Peterson, G. A. et al. Demonstration of efficient nonreciprocity in a microwave optomechanical circuit. *Phys. Rev. X* **7**, 031001 (2017).
- Metelmann, A. & Clerk, A. A. Nonreciprocal photon transmission and amplification via reservoir engineering. *Phys. Rev. X* **5**, 021025 (2015).
- Fang, K. J. et al. Generalized non-reciprocity in an optomechanical circuit via synthetic magnetism and reservoir engineering. *Nat. Phys.* **13**, 465–471 (2017).
- Xu, H. et al. Nonreciprocal control and cooling of phonon modes in an optomechanical system. *Nature* **568**, 65–69 (2019).
- Wang, Y. P. et al. Nonreciprocity and unidirectional invisibility in cavity magnonics. *Phys. Rev. Lett.* **123**, 127202 (2019).
- Fang, K. J., Yu, Z. F. & Fan, S. H. Realizing effective magnetic field for photons by controlling the phase of dynamic modulation. *Nat. Photonics* **6**, 782–787 (2012).
- Fang, K. J. & Fan, S. H. Controlling the flow of light using the inhomogeneous effective gauge field that emerges from dynamic modulation. *Phys. Rev. Lett.* **111**, 203901 (2013).
- Xia, K. Y., Nori, F. & Xiao, M. Cavity-free optical isolators and circulators using a chiral cross-Kerr nonlinearity. *Phys. Rev. Lett.* **121**, 203602 (2018).
- Zhang, S. C. et al. Thermal-motion-induced non-reciprocal quantum optical system. *Nat. Photonics* **12**, 744–748 (2018).
- Haldane, F. D. M. & Raghu, S. Possible realization of directional optical waveguides in photonic crystals with broken time-reversal symmetry. *Phys. Rev. Lett.* **100**, 013904 (2008).
- Bi, L. et al. On-chip optical isolation in monolithically integrated non-reciprocal optical resonators. *Nat. Photonics* **5**, 758–762 (2011).
- Hadad, Y. & Steinberg, B. Z. Magnetized spiral chains of plasmonic ellipsoids for one-way optical waveguides. *Phys. Rev. Lett.* **105**, 233904 (2010).
- Khanikaev, A. B. et al. One-way extraordinary optical transmission and non-reciprocal spoof plasmons. *Phys. Rev. Lett.* **105**, 126804 (2010).
- Yu, Z. F. & Fan, S. H. Complete optical isolation created by indirect interband photonic transitions. *Nat. Photonics* **3**, 91–94 (2009).
- Kang, M. S., Butsch, A. & Russell, P. S. J. Reconfigurable light-driven opto-acoustic isolators in photonic crystal fibre. *Nat. Photonics* **5**, 549–553 (2011).
- Tzuang, L. D. et al. Non-reciprocal phase shift induced by an effective magnetic flux for light. *Nat. Photonics* **8**, 701–705 (2014).
- Estep, N. A. et al. Magnetic-free non-reciprocity and isolation based on parametrically modulated coupled-resonator loops. *Nat. Phys.* **10**, 923–927 (2014).
- Koutserimpas, T. T. & Fleury, R. Nonreciprocal gain in non-Hermitian time-floquet systems. *Phys. Rev. Lett.* **120**, 087401 (2018).
- Kittlaus, E. A. et al. Non-reciprocal interband Brillouin modulation. *Nat. Photonics* **12**, 613–619 (2018).
- Guo, X. X. et al. Nonreciprocal metasurface with space-time phase modulation. *Light. Sci. Appl.* **8**, 123 (2019).
- Khanikaev, A. B. & Alù, A. Optical isolators: nonlinear dynamic reciprocity. *Nat. Photonics* **9**, 359–361 (2015).
- Shi, Y., Yu, Z. F. & Fan, S. H. Limitations of nonlinear optical isolators due to dynamic reciprocity. *Nat. Photonics* **9**, 388–392 (2015).
- Dai, D. X., Bauters, J. & Bowers, J. E. Passive technologies for future large-scale photonic integrated circuits on silicon: polarization handling, light non-reciprocity and loss reduction. *Light. Sci. Appl.* **1**, e1 (2012).
- Sounas, D. L. & Alù, A. Non-reciprocal photonics based on time modulation. *Nat. Photonics* **11**, 774–783 (2017).
- Vahala, K. J. Optical microcavities. *Nature* **424**, 839–846 (2003).
- You, J. Q. & Nori, F. Atomic physics and quantum optics using superconducting circuits. *Nature* **474**, 589–597 (2011).
- Aspelmeyer, M., Kippenberg, T. J. & Marquardt, F. Cavity optomechanics. *Rev. Mod. Phys.* **86**, 1391–1452 (2014).

44. Hammerer, K, Sørensen, A. S. & Polzik, E. S. Quantum interface between light and atomic ensembles. *Rev. Mod. Phys.* **82**, 1041–1093 (2010).
45. Liu, Y. C. et al. Coherent polariton dynamics in coupled highly dissipative cavities. *Phys. Rev. Lett.* **112**, 213602 (2014).
46. Yang, F., Liu, Y. C. & You, L. Anti-PT symmetry in dissipatively coupled optical systems. *Phys. Rev. A* **96**, 053845 (2017).
47. Feng, L., El-Ganainy, R. & Ge, L. Non-Hermitian photonics based on parity-time symmetry. *Nat. Photonics* **11**, 752–762 (2017).
48. Peng, B. et al. Loss-induced suppression and revival of lasing. *Science* **346**, 328–332 (2014).
49. Sato, Y. et al. Strong coupling between distant photonic nanocavities and its dynamic control. *Nat. Photonics* **6**, 56–61 (2012).
50. Xiao, Y. F. et al. Asymmetric Fano resonance analysis in indirectly coupled microresonators. *Phys. Rev. A* **82**, 065804 (2010).
51. Weidemann, S. et al. Topological funneling of light. *Science* **368**, 311–314 (2020).